

Brief Articles

Macrocyclization in the Design of Non-Phosphorus-Containing Grb2 SH2 Domain-Binding Ligands

Zhen-Dan Shi,[†] Chang-Qing Wei,[†] Kyeong Lee,[†] Hongpeng Liu,[‡] Manchao Zhang,[‡] Toshiyuki Araki,[§] Lindsey R. Roberts,[#] Karen M. Worthy,[#] Robert J. Fisher,[#] Benjamin G. Neel,[§] James A. Kelley,[†] Dajun Yang,[‡] and Terrence R. Burke, Jr.*[†]

Laboratory of Medicinal Chemistry, CCR, National Cancer Institute, National Institutes of Health, Frederick, Maryland 21702, University of Michigan Medical School, Ann Arbor, Michigan 48109, Beth Israel Deaconess Medical Center, Boston, Massachusetts 02215, and Protein Chemistry Laboratory, SAIC–Frederick, Frederick, Maryland 21702

Received October 8, 2003

Macrocyclization from the phosphotyrosyl (pTyr) mimetic's β -position has previously been shown to enhance Grb2 SH2 domain-binding affinity of phosphonate-based analogues. The current study examined the effects of such macrocyclization using a dicarboxymethyl-based pTyr mimetic. In extracellular assays affinity was enhanced approximately 5-fold relative to an open-chain congener. Enhancement was also observed in whole-cell assays examining blockade of Grb2 binding to the erbB-2 protein-tyrosine kinase.

In our efforts to develop Grb2 SH2 domain-signaling antagonists, we have examined non-phosphorus-containing, carboxy-based pTyr mimetics displayed in a high-affinity Grb2 SH2 domain-binding platform (**1a**, Figure 1) first disclosed by Novartis Corporation.¹ Of several carboxy-based analogues,^{2–5} the greatest potency was obtained using a 4-malonylphenylalanine residue bearing an *N*^ε-oxalyl substituent (**1b**).⁴ In separate work using phosphonate-containing pTyr mimetics, recently we have employed ring-closing olefin metathesis (RCM) to prepare macrocyclic tetrapeptide mimetics of type **2** as globally constrained congeners that exhibited enhanced Grb2 SH2 domain-binding potency and efficacy in whole cells.⁶ However, it had remained to be shown what the combined effects of macrocyclization would be in conjunction with carboxy-based pTyr mimetics, since macrocycle-induced alterations of binding within the pTyr pocket could potentially have unexpected results. To address these uncertainties, reported herein is a non-phosphorus-containing macrocycle (**3** and its sodium salt **3s**) along with biological evaluation in both in vitro and in vivo systems.

Synthesis

Synthesis of the final product **3** was by a procedure similar to that recently reported for the preparation of the analogous phosphonate-containing macrocycle **2**.⁶ Preparation of the required tri-(*O*Bu)⁴-containing **10** was achieved as shown in Scheme 1.

Results and Discussion

To approximate potential binding interactions of macrocycle **3** with the Grb2 SH2 domain, molecular

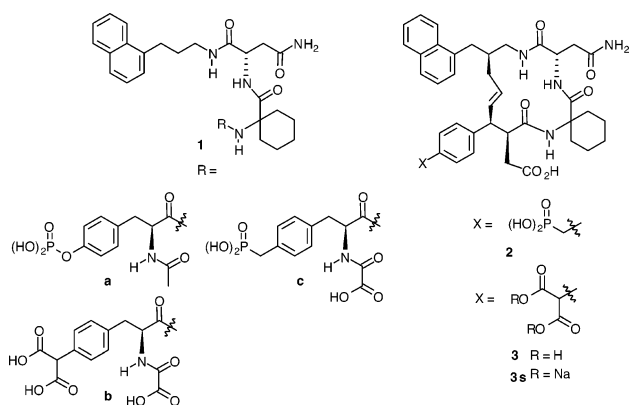


Figure 1. Structures of open-chain and macrocyclic Grb2 SH2 domain-binding analogues.

modeling studies were carried out using the previously reported X-ray structure of a phosphohexapeptide bound to the Grb2 SH2 domain.⁷ Low-energy binding modes were compared for the open-chain **1b** and its corresponding macrocycle **3** (Figure 2). Significant differences were noted in the hydrogen-bonding interactions of certain oxygens comprising the phosphate-mimicking malonyl groups. It was found that the malonyl group of macrocycle **3** did not fully participate in the network of hydrogen bonds within the pTyr pocket that were displayed by **1b**.

Measurement of in Vitro Grb2 SH2 Domain-Binding Affinity. By use of extracellular ELISA-based Grb2 SH2 domain binding assays,^{4,6} open-chain analogues **1b** and **1c** were compared with their corresponding macrocyclic congeners **3s** and **2**, respectively (Table 1). The IC₅₀ values obtained for **1b**, **1c**, and **2** (22, 10, and 1.4 nM, respectively) were of the same order as the previously reported data (70,⁴ 9,⁸ and 2,⁶ respectively). The newly prepared macrocycle **3s** exhibited an IC₅₀ of 4.3 ± 2.4 nM, which is approximately 5-fold more potent

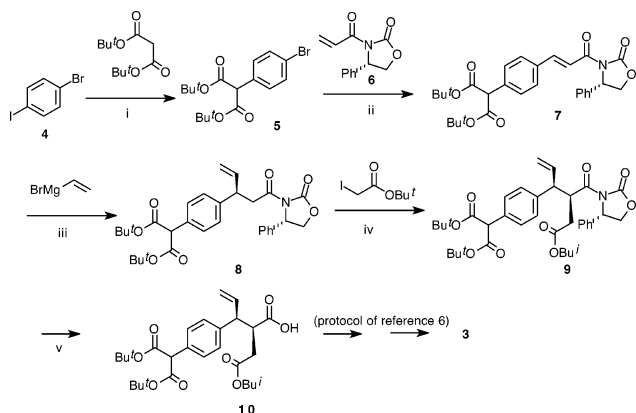
* To whom correspondence should be addressed. Phone: (301) 846-5906. Fax: (301) 846-6033. E-mail: tburke@helix.nih.gov.

[†] National Cancer Institute.

[‡] University of Michigan Medical School.

[§] Beth Israel Deaconess Medical Center.

[#] SAIC–Frederick.

Scheme 1^a

^a Reagents and conditions: (i) NaH, CuBr, dioxane, HMPA, reflux, 3 h (75% yield); (ii) Pd(OAc)₂, (*o*-tolyl)₃P, Et₃N, reflux, 16 h (87% yield); (iii) PhSCu, Et₂O, THF, -40 °C, 3 h (58% yield) [73% de]; (iv) NaHMDS, THF, -78 °C, 2 h (53% yield); (v) LiOH, H₂O₂, 0 °C, 2.5 h, then room temp, 2.5 h (73% yield).

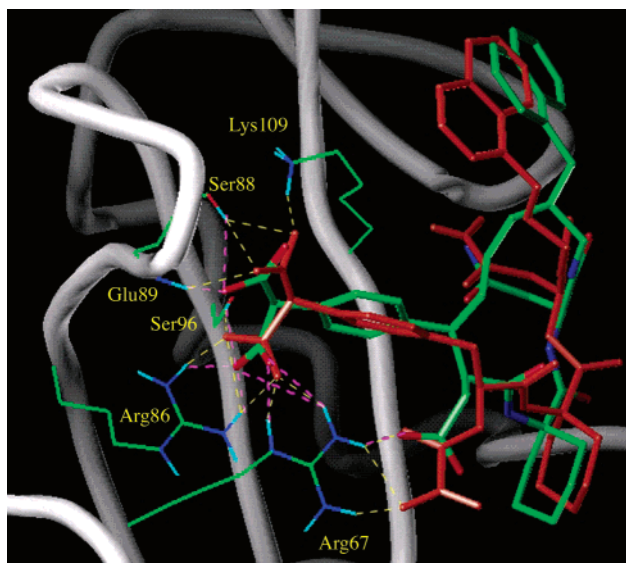


Figure 2. Molecular modeling overlay of **1b** and **3s** complexed to the Grb2 SH2 domain with protein backbone atoms superimposed. Ligands are shown in larger diameter stick rendering with **1b** colored red and **3s** colored by atom, with green being carbon. For clarity, protein and amino acid side chains/backbone amides for the **1b** complex only are shown. Hydrogen bonds are represented as dashed lines (yellow for protein-**1b** and pink for protein-**3s**).

than its open-chain homologue **1b**. To our knowledge, **3s** is the most potent non-phosphorus-containing Grb2 SH2 domain-binding antagonist reported to date. Surface plasmon resonance (SPR) derived K_d measurement, determined by analyzing the direct binding of synthetic compounds to Grb2 SH2 domain protein, provided K_d values for **1c** and **2** of 128⁹ and 0.9 nM,⁹ respectively

Table 1. Grb2 SH2 Domain-Binding Affinities Determined by SPR and ELISA Techniques

compd	SPR-derived ^a			ELISA-derived ^a IC ₅₀ ± SD (nM)
	k_{on} (M ⁻¹ s ⁻¹)	k_{off} (s ⁻¹)	K_d ± SD (nM)	
1b	rapid equilibrium			22.1 ± 7.1 (<i>n</i> = 5)
1c	8.9 × 10 ⁵	1.1 × 10 ⁻¹	128.1 ± 92.9 (<i>n</i> = 8) ^b	10.0 ± 4.8 (<i>n</i> = 3)
2	6.7 × 10 ⁶	5.6 × 10 ⁻³	0.9 ± 0.4 (<i>n</i> = 4) ^b	1.4 ± 0.7 (<i>n</i> = 4)
3s	5.5 × 10 ⁶	4.4 × 10 ⁻²	12.1 ± 9.8 (<i>n</i> = 10)	4.3 ± 2.4 (<i>n</i> = 8)

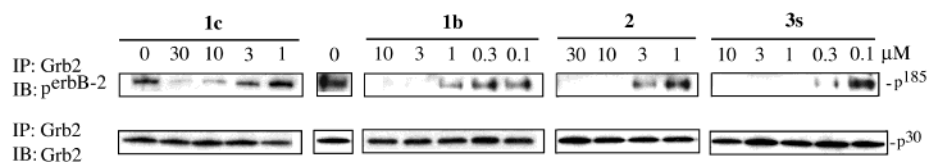
^a Values were determined as outlined in the Experimental Section. ^b Previously reported in ref 9.

(Table 1). The K_d value obtained for macrocycle **2** compared favorably with affinity as determined above by ELISA techniques (IC₅₀ = 1.4 nM). Similarly, the K_d value for **1c** was of the same order as the IC₅₀ value previously obtained using SPR (IC₅₀ ≈ 80 nM).² Surprisingly, however, the SPR value for open-chain **1c** was significantly higher (~10-fold) than the ELISA-derived IC₅₀ value (10.0 ± 4.8 nM, Table 1). As with macrocycle **2**, the SPR-derived K_d value for macrocycle **3s** (12.1 nM) was only slightly higher than the corresponding ELISA-derived IC₅₀ value (4 nM). Undesirably fast off rates were observed despite high affinity, consistent with previous reports that fast off rates are characteristic of SH2 domain-binding pTyr-containing peptides.¹⁰

Inhibition of Grb2 Binding to p185^{erbB-2} in Cells in Culture. Affinity constants obtained by in vitro methods may not accurately reflect behavior in whole cells, where passage across lipid bilayers must occur prior to competing with phosphorylated protein ligand for binding to Grb2 SH2 domains. Therefore, studies were conducted by treating cells with varying concentrations of **1b**, **1c**, **2**, and **3s** in solution and then measuring the levels of intracellular association of Grb2 with cytoplasmic erbB-2 PTK (in MDA-MB-453 breast cancer cells). As shown in Figure 3, the greater potency of **2** relative to **1c** is consistent with those from previous reports.⁶ A comparison of data for **3s** versus **1b** indicates that the same can now be concluded for non-phosphorus-containing macrocycles, namely, that macrocyclization enhances apparent Grb2 SH2 domain inhibitory potency in whole cell systems.

Conclusions

The intent of the current study was to examine the effects of macrocyclization on a non-phosphorus-containing, carboxy-based ligand where the effects of conformational constraints on binding orientations within the critical pTyr-binding pocket were unknown. Resultant affinity enhancements in both extracellular and whole-cell assays further validated the potential utility of macrocyclization in the design of Grb2 SH2 domain-binding antagonists.



Panel B

Figure 3. Inhibition of Grb2 binding in whole cells. Anti-phosphotyrosine Western blots of MDA-MB-453 breast cancer cell lysates following treatment with analogues **1b**, **1c**, **2**, and **3s** at the indicated concentrations, cell lysis, and immunoprecipitation with Grb2 polyclonal antibody. Probing of the same blot with Grb2 MAb was performed as control.

Experimental Section

Molecular Modeling. Molecular modeling studies were carried out using MacroModel 8.0 (Schrödinger, L.L.C.) and Sybyl 6.9 (Tripos, Inc.) on a Silicon Graphics Octane 2 workstation. Construction of the protein–ligand complexes was based on the X-ray structure of the Grb2 SH2 domain complexed with a hexapeptide inhibitor (PDB entry 1TZE).⁷ The complex structure was minimized on MacroModel using MMFF94s force field with a continuum solvation model. The SD method was used with convergence criteria set to Gradient. Ligand and protein residues within 5 Å were allowed to move freely during energy minimization, while residues at a distance between 5 and 10 Å were constrained by a parabolic force constant of 50 kJ/Å. Residues beyond 10 Å were frozen. Results are shown in Figure 2.

Extracellular Binding Assays. Plasmon resonance analyses of antagonist binding to Grb2 SH2 domain protein were performed on BIACORE 2000 and BIACORE 3000 instruments (Biacore Inc., Piscataway NJ). Data were fit to a simple 1:1 interaction model with a correction for mass transport using the global data analysis program CLAMP.¹¹ Results are shown in Table 1. Experimental details are contained in the Supporting Information. ELISA-based binding assays were as conducted as previously reported.⁴ Results are shown in Table 1.

Inhibition of Grb2 SH2 Domain Binding in Whole Cells. Analyses of Grb2 binding to p185^{erbB-2} in erbB-2 overexpressing MDA-MB-453 breast cancer cells were conducted as previously reported.⁴ Results are shown in Figure 3.

2-(4-Bromophenyl)propane-1,3-dioic Acid Bis(1,1-dimethylethyl) Ester (5). To a suspension of sodium hydride, 60% in oil (1.88 g, 46.9 mmol) in anhydrous dioxane (80 mL), was added hexamethylphosphoramide (HMPA) (6 mL) and di-*tert*-butyl malonate (10.14 g, 46.9 mmol). The mixture was stirred at room temperature (1 h), charged with copper(I) bromide (8.08 g, 56.3 mmol) and 1-bromo-4-iodobenzene (4) (15.00 g, 53.02 mmol), and refluxed under argon (3 h). After cooling to room temperature, the mixture was subjected to an extractive workup and purified by silica gel flash chromatography to provide **5** as a white solid (13.22 g, 75% yield). ¹H NMR (CDCl₃) δ 7.47 (dd, 2 H, *J* = 6.66 and 2.0 Hz), 7.26 (dd, 2H, *J* = 6.5 and 1.9 Hz), 4.40 (s, 1H), 1.46 (s, 18H). FABMS *m/z* 371 [MH⁺]. Anal. (C₁₇H₂₃O₄Br) C, H.

2-{4-[(1*E*)-3-((4*S*)-2-Oxo-4-phenyl(1,3-oxazolidin-3-yl))-3-oxoprop-1-enyl]phenyl}propane-1,3-dioic Acid Bis(1,1-dimethylethyl) Ester (7). To a solution of **5** (7.77 g, 20.95 mmol) and (4*S*)-3-(1-oxo-2-propenyl)-4-phenyl-2-oxazolidinone (**6**)⁶ (4.55 g, 20.95 mmol) in Et₃N (87 mL) was added Pd(OAc)₂ (233 mg, 0.993 mmol) and (*o*-tolyl)₃P (1.30 g, 4.27 mmol). The mixture was refluxed under argon (16 h), then cooled to room temperature, diluted with CH₂Cl₂, and filtered through Celite. The mixture was subjected to an extractive workup and purified by silica gel flash chromatography to provide **7** as a white solid (9.19 g, 87% yield). ¹H NMR (CDCl₃) δ 7.91 (d, 1H, *J* = 15.6 Hz), 7.76 (d, 1H, *J* = 15.6 Hz), 7.56 (d, 2H, *J* = 8.4 Hz), 7.41–7.33 (m, 7H), 5.55 (dd, 1H, *J* = 4.0 and 8.8 Hz), 4.73 (t, 1H, *J* = 8.8 Hz), 4.43 (s, 1H), 4.31 (*J* = 4.0 and 8.8 Hz), 1.45 (s, 18H). FABMS *m/z* 508 [MH⁺]. Anal. (C₂₉H₃₅NO₇·0.25H₂O) C, H, N.

2-{4-[(1*R*)-3-((4*S*)-2-Oxo-4-phenyl(1,3-oxazolidin-3-yl))-3-oxo-1-vinylpropyl]phenyl}propane-1,3-dioic Acid Bis(1,1-dimethylethyl) Ester (8). To a slurry of PhSCu (3.10 g, 17.94 mmol) in dry ether (250 mL) under argon at –40 °C was added dropwise a solution of vinylmagnesium bromide, 1.0 M in THF (53.8 mL, 53.8 mmol), over 40 min. The mixture was stirred at –40 °C (20 min), a precooled solution of **7** (9.10 g, 17.94 mmol) in THF (150 mL) was added over 1 h, and the resulting mixture was stirred at –40 °C (3 h). The mixture was subjected to an extractive workup and purified by silica gel flash chromatography to provide **8** as a yellow solid (5.60 g, 58% yield). ¹H NMR (CDCl₃) δ 7.36–7.20 (m, 9H), 5.96 (ddd, 1H, *J* = 7.0, 10.5, and 17.0 Hz), 5.29 (dd, 1H, *J* = 3.3 and 8.6 Hz), 5.00–4.94 (m, 2H), 4.57 (t, 1H, *J* = 8.7 Hz), 4.40 (s, 1H),

4.21 (dd, 1H, *J* = 3.3 and 8.8 Hz), 3.90 (m, 1H), 3.52 (dd, 1H, *J* = 8.3 and 16.5 Hz), 3.31 (dd, 1H, *J* = 6.6 and 16.4 Hz), 1.47 (s, 18H). FABMS *m/z* 536 [MH⁺]. Anal. (C₃₁H₃₇NO₇) C, H, N.

2-[4-(3-((4*S*)-2-Oxo-4-phenyl(1,3-oxazolidin-3-yl))(1*S*,2*S*)-2-[(*tert*-butyl)oxycarbonylmethyl]-3-oxo-1-vinylpropyl)-phenyl]propane-1,3-dioic Acid Bis(1,1-dimethylethyl) Ester (9). To a 1 M stirred solution of *N*-sodiohexamethyl-disilazane (NaHMDS) in THF (24.00 mL, 24.00 mmol) was added dropwise a solution of **8** (5.58 g, 10.4 mmol) in THF (60 mL) at –78 °C. The solution was stirred at –78 °C (1 h), then iodoacetate *tert*-butyl ester (2.55 g, 10.5 mmol) in THF (30 mL) was added, and the mixture was stirred for an additional 4 h at –78 °C. The mixture was subjected to an extractive workup and purified by silica gel flash chromatography to provide **9** as a colorless oil (3.60 g, 53% yield). ¹H NMR (CDCl₃) δ 7.43–7.22 (m, 9H), 6.08 (m, 1H), 5.21–5.17 (m, 2H), 4.83–4.76 (m, 2H), 4.41 (s, 1H), 3.97 (t, 1H, *J* = 8.4 Hz), 3.86 (dd, 1H, *J* = 2.5 and 8.6 Hz), 3.32 (t, 1H, *J* = 10.0 Hz), 2.77 (dd, 1H, *J* = 11.3 and 17.2 Hz), 2.64 (dd, 1H, *J* = 3.7 and 17.2 Hz), 1.47 (s, 18H), 1.31 (s, 9H). FABMS *m/z* 650 [MH⁺]. HRFAB-MS calcd for C₂₉H₃₂O₉N (MH⁺ – 2C₄H₈): 538.2077. Found: 538.2022.

(2*S*,3*S*)-3-(4-Bis[(*tert*-butyl)oxycarbonylmethyl]-phenyl)-2-[(*tert*-butyl)oxycarbonylmethyl]pent-4-enoic Acid (10). A solution of 30% H₂O₂ (2.80 mL, 27.5 mmol) was added via syringe over 10 min to a solution of **9** (3.58 g, 5.51 mmol) in THF/H₂O (v:v, 3:1) (84 mL) at 0 °C. This was followed by addition of LiOH (463 mg, 11.03 mmol) in H₂O (11 mL). After being stirred at 0 °C for 2.5 h, the solution was warmed to room temperature and stirring was continued for an additional 2.5 h. Sodium sulfite (3.47 g, 27.5 mmol) in H₂O (23 mL) was added to the mixture followed by addition of 1 N HCl (27 mL). Evaporation of solvent in vacuo provided a residue, which was subjected to an extractive workup and purified by silica gel flash chromatography to give **10** as a yellow solid (2.02 g, 73% yield). ¹H NMR (CDCl₃) δ 7.32 (d, 2H, *J* = 8.4 Hz), 7.21 (d, 2H, *J* = 8.2 Hz), 5.95 (m, 1H), 5.17–5.13 (m, 2H), 4.40 (s, 1H), 3.68 (t, 1H, *J* = 8.6 Hz), 3.23 (m, 1H), 2.63 (dd, 1H, *J* = 10.7 and 16.8 Hz), 2.44 (dd, 1H, *J* = 3.9 and 17.0 Hz), 1.46 (s, 18H), 1.28 (s, 9H). FABMS (negative ion) *m/z* 503 [M – H][–]. Anal. (C₂₈H₄₀O₈·1.25H₂O) C, H.

Acknowledgment. T.A. is a Fellow of the Leukemia and Lymphoma Society (Grant No. 5094-03). Work was supported in part by NIH Grant R01 CA49152 (to B.G.N.).

Supporting Information Available: Detailed experimental protocols for SPR binding analysis as well as the detailed modifications of procedures in ref 6 used to prepare macrocycle **3** from pTyr mimetic **10**. This material is available free of charge via the Internet at <http://pubs.acs.org>.

References

- Furet, P.; Gay, B.; Caravatti, G.; Garcia-Echeverria, C.; Rahuel, J.; Schoepfer, J.; Fretz, H. Structure-based design and synthesis of high affinity tripeptide ligands of the Grb2-SH2 domain. *J. Med. Chem.* **1998**, *41*, 3442–3449.
- Yao, Z. J.; King, C. R.; Cao, T.; Kelley, J.; Milne, G. W. A.; Voigt, J. H.; Burke, T. R. Potent inhibition of Grb2 SH2 domain binding by non-phosphate-containing ligands. *J. Med. Chem.* **1999**, *42*, 25–35.
- Burke, T. R., Jr.; Luo, J.; Yao, Z.-J.; Gao, Y.; Milne, G. W. A.; Guo, R.; Voigt, J. H.; King, C. R.; Yang, D. Monocarboxylic phosphotyrosyl mimetics in the design of Grb2 SH2 domain inhibitors. *Bioorg. Med. Chem. Lett.* **1999**, *9*, 347–352.
- Gao, Y.; Luo, J.; Yao, Z.-J.; Guo, R.; Zou, H.; Kelley, J.; Voigt, J. H.; Yang, D.; Burke, T. R., Jr. Inhibition of Grb2 SH2 domain binding by non-phosphate containing ligands. 2. 4-(2-Malonyl)-phenylalanine as a potent phosphotyrosyl mimetic. *J. Med. Chem.* **2000**, *43*, 911–920.
- Burke, T. R., Jr.; Yao, Z. J.; Gao, Y.; Wu, J. X.; Zhu, X.; Luo, J. H.; Guo, R.; Yang, D. N-Terminal carboxyl and tetrazole-containing amides as adjuvants to Grb2 SH2 domain ligand binding. *Bioorg. Med. Chem.* **2001**, *9*, 1439–1445.
- Wei, C.-Q.; Gao, Y.; Lee, K.; Guo, R.; Li, B.; Zhang, M.; Yang, D.; Burke, T. R., Jr. Macrocyclization in the design of Grb2 SH2 domain-binding ligands exhibiting high potency in whole cell systems. *J. Med. Chem.* **2003**, *46*, 244–254.

- (7) Rahuel, J.; Gay, B.; Erdmann, D.; Strauss, A.; GarciaEcheverria, C.; Furet, P.; Caravatti, G.; Fretz, H.; Schoepfer, J.; Grutter, M. G. Structural basis for specificity of GRB2-SH2 revealed by a novel ligand binding mode. *Nat. Struct. Biol.* **1996**, *3*, 586–589.
- (8) Wei, C.-Q.; Li, B.; Guo, R.; Yang, D.; Burke, T. R., Jr. Development of a phosphatase-stable phosphotyrosyl mimetic suitably protected for the synthesis of high affinity Grb2 SH2 domain-binding ligands. *Bioorg. Med. Chem. Lett.* **2002**, *12*, 2781–2784.
- (9) Shi, Z.-D.; Lee, K.; Liu, H.; Zhang, M.; Roberts, L. R.; Worthy, K. M.; Fivash, M. J.; Fisher, R. J.; Yang, D.; Burke, T. R., Jr. A novel macrocyclic tetrapeptide mimetic that exhibits low-picomolar Grb2 SH2 domain-binding affinity. *Biochem. Biophys. Res. Commun.* **2003**, *310*, 378–383.
- (10) Felder, S.; Zhou, M.; Hu, P.; Urena, J.; Ullrich, A.; Chaudhuri, M.; White, M.; Shoelson, S. E.; Schlessinger, J. SH2 domains exhibit high-affinity binding to tyrosine-phosphorylated peptides yet also exhibit rapid dissociation and exchange. *Mol. Cell. Biol.* **1993**, *13*, 1449–1455.
- (11) Myszka, D. G.; Morton, T. A. CLAMP: a biosensor kinetic data analysis program. *Trends Biochem. Sci.* **1998**, *23*, 149–150.

JM030510E